ELSEVIER

Journal of Contaminant Hydrology 26 (1997) 279–289

JOURNAL OF
Contaminant
Hydrology

Intercomparison between TRIO-EF and IMPACT codes with reference to experimental strontium migration data

L. Trotignon [a,*], M.-H. Fauré [b], A. Stietel [c], C. Riglet-Martial [a], M. Sardin [d], P. Vitorge [b], F. Lefèvre [b]

[a] *CEA DCC / DESD / SESD / Section de Géosciences et d'Expérimentations, C.E. Cadarache, 13108 Saint-Paul-lez-Durance Cédex, France*

[b] *CEA DCC / DESD / SESD / Section de GéoChimie, C.E. Fontenay-aux-Roses, BP 6, 92265 Fontenay-aux-Roses Cédex, France*

[c] *CEA DRN / DMT / SEMT / Laboratoire TTMF, C.E. Saclay, 91191 Gif-sur-Yvette Cédex, France*

[d] *CNRS LSGC-ENSIC, 1 rue Grandville, BP 451, 54001 Nancy Cédex, France*

Received 15 March 1996; accepted 15 August 1996

Abstract

This work presents an intercomparison exercise between two geochemical migration codes, TRIO-EF (an object-oriented finite element code) and IMPACT (a chemical engineering code using mixing cells in series). The predictions of the two codes are compared with the reference experimental results obtained in a previous study of strontium transport in soil columns. This simulated geochemical system is well documented and includes ion exchange and dissolution–precipitation reactions. The solution transport is simulated by a one-dimensional advection–dispersion model. The predictions of TRIO-EF and IMPACT are both in good agreement with the experimental results. However, slight differences can be observed between the two codes, especially when concentration discontinuities are involved, such as precipitation fronts or changes in boundary conditions. These discrepancies between the two codes can mainly be attributed to the different discretisation approaches. © 1997 Elsevier Science B.V.

Keywords: Calcium; Clay; Ion-exchange; Migration codes; Precipitation; Strontium

* Corresponding author.

PII S0169-7722(96)00075-7

1. Introduction

The performance assessment of nuclear waste disposal requires in particular quantitative predictions of the radioelement migration through the geological environment. The standard K_d partition coefficient approach, used to account for reversible sorption or ion-exchange reactions of species at low concentrations, is not sufficient when the chemical conditions vary during transport (dissolution–precipitation, pH fronts, etc.) as in many natural systems. Migration codes which include a more detailed description of the chemical processes occurring during transport have been developed in order to overcome this limitation. An important stage of this development work consists in evaluating the reliability of the codes. This can be achieved by the comparison of experimental data with the code predictions.

The aim of this work is to compare, on the basis of dedicated migration experiments, the predictions of two coupled transport-chemistry codes, TRIO-EF and IMPACT, which solve migration problems with different numerical methods. The reference migration experiments used in this exercise (Lefèvre et al., 1993) display multiple physico-chemical phenomena (ion exchange, complexation and precipitation) for a well-documented chemical system. This previous work also included the IMPACT computations of the results. In the first part of the present paper, the experimental results are recalled and a summary of the conceptual model is given. Then, a description of the TRIO-EF and IMPACT codes is made. The predictions of the two codes for the reference experiments are then compared and discussed.

2. Reference experiments and conceptual models

2.1. Experiments

The intercomparison exercise is based on the experimental results on strontium migration which were discussed in a previous paper (Lefèvre et al., 1993). Two reference experiments are considered in this paper: the SOLEX experiment which involves both the ion exchange phenomena and the dissolution–precipitation reactions, and the IONEX experiment in which operating conditions exclude the dissolution–pre-

Table 1
SOLEX and IONEX reference experiments: chemical composition of the pre-equilibration, injection and elution solutions. V_p is the porous volume of the column (26 ml)

Experiment	Pre-equilibrating solution	Injection solution		Elution solution
		Volume	Composition	
SOLEX	water	$2V_p$	$SrCl_2$ 7.15×10^{-5} M	$CaCl_2$ 4.63×10^{-3} M
IONEX	$CaCl_2$ 4.69×10^{-3} M	$2V_p$	$SrCl_2$ 9.3×10^{-5} M $CaCl_2$ 4.69×10^{-3} M	$CaCl_2$ 4.69×10^{-3} M

cipitation of $SrCO_{3s}$ so that the retardation of strontium is only due to the Sr^{++}/Ca^{++} ion exchange phenomena. The experimental conditions are summarised in Table 1. The soil sample (Güe sand) used for the transport experiments is a clayey sand containing small amounts of calcite. After equilibrating the column with deionised water (SOLEX) or a $CaCl_2$ solution (IONEX), a definite volume of an $SrCl_2$ solution is injected. Then, the composition of the feeding solution is changed in order to elute the fixed and/or precipitated strontium. Table 2 reports, for the two reference experiments, the measurements of the dissolved concentrations of Sr and Ca at the outlet of the column. The relative uncertainty regarding the experimental results is estimated to be less than 5% except at the tail of the elution peak ($< 10\%$). There are no experimental data on the spatial distribution of the chemical elements in the column.

Table 2
Experimental data for SOLEX (ion exchange + precipition) and IONEX (ion exchange only) experiments. The concentrations of Sr and Ca at the column outlet are given as a function of the reduced elution volume. A relative uncertainty on values is estimated to be less than 5%

SOLEX experiment			IONEX experiment		
V/V_p	Sr^{2+} (M)	Ca^{2+} (M)	V/V_p	Sr^{2+} (M)	Ca^{2+} (M)
0.33	0		0.34	0	4.84×10^{-3}
0.66	0	5.07×10^{-5}	0.68	0	4.69×10^{-3}
0.99	0	5.55×10^{-5}	1.02	0	4.73×10^{-3}
1.32	0	9.87×10^{-5}	1.39	0	4.88×10^{-3}
1.65	0	1.12×10^{-4}	1.70	0	4.79×10^{-3}
1.96	0	1.07×10^{-4}	2.03	0	4.81×10^{-3}
2.29	0	9.89×10^{-5}	2.38	0	4.86×10^{-3}
2.62	0	9.93×10^{-5}	2.71	0	4.77×10^{-3}
2.95	0	1.11×10^{-4}	3.05	0	4.85×10^{-3}
3.28	0	2.69×10^{-3}	3.40	0	4.77×10^{-3}
3.61	0	4.75×10^{-3}	3.72	4.25×10^{-6}	4.79×10^{-3}
3.94	0	4.68×10^{-3}	4.07	2.91×10^{-5}	4.70×10^{-3}
4.27	0	4.75×10^{-3}	4.41	6.22×10^{-5}	4.79×10^{-3}
4.60	0	4.73×10^{-3}	4.75	7.95×10^{-5}	4.76×10^{-3}
4.93	0	4.73×10^{-3}	5.09	8.58×10^{-5}	4.90×10^{-3}
5.26	0	4.73×10^{-3}	5.43	8.84×10^{-5}	4.79×10^{-3}
5.59	8.50×10^{-6}	4.78×10^{-3}	5.77	8.28×10^{-5}	4.80×10^{-3}
5.93	6.82×10^{-5}	4.68×10^{-3}	6.11	6.18×10^{-5}	4.69×10^{-3}
6.26	1.26×10^{-4}	4.65×10^{-3}	6.45	3.61×10^{-5}	4.84×10^{-3}
6.59	8.87×10^{-5}	4.64×10^{-3}	6.73	1.88×10^{-5}	4.79×10^{-3}
6.92	5.26×10^{-5}	4.62×10^{-3}	7.07	1.01×10^{-5}	4.99×10^{-3}
7.25	2.88×10^{-5}	4.70×10^{-3}	7.39	5.57×10^{-6}	4.93×10^{-3}
7.58	1.55×10^{-5}	4.66×10^{-3}	7.73	3.37×10^{-6}	5.18×10^{-3}
7.91	8.82×10^{-6}	4.66×10^{-3}	8.06	2.18×10^{-6}	5.18×10^{-3}
8.25	5.27×10^{-6}	4.66×10^{-3}			
8.58	3.38×10^{-6}	4.64×10^{-3}			
8.91	2.25×10^{-6}	4.70×10^{-3}			
9.23	1.46×10^{-6}	4.69×10^{-3}			
9.56	1.05×10^{-6}	4.67×10^{-3}			
9.89	1.23×10^{-6}	4.61×10^{-3}			

Table 3
Chemical reactions and associated values of equilibrium constants (molar scale) at zero ionic strength and $T = 298$ K. $H_2CO_3^*$ accounts for both dissolved CO_2 and non-dissociated H_2CO_3. Subscripts "s" and "f" stand for the solid and adsorbed species. The selectivity factor $K_{Sr/Ca}$ for the Sr^{2+}/Ca^{2+} ion exchange is defined by $K_{Sr/Ca} = \dfrac{[Ca^{++}][Sr_f^{++}]}{[Sr^{++}][Ca_f^{++}]} = 1.05$

Reaction	Equilibrium constant
$H_2O \Leftrightarrow H^+ + OH^-$	$\log(K_w) = -14$
$H_2CO_3^* \Leftrightarrow HCO_3^- + H^+$	$\log(K_1) = -6.3$
$HCO_3^- \Leftrightarrow CO_3^{2-} + H^+$	$\log(K_2) = -10.3$
$CO_2(g) + H_2O \Leftrightarrow H_2CO_3^*$	$\log(K_p) = -1.47$
$CaCO_{3s} \Leftrightarrow Ca^{2+} + CO_3^{2-}$	$\log(K_{s1}) = -8.42$
$SrCO_{3s} \Leftrightarrow Sr^{2+} + CO_3^{2-}$	$\log(K_{s2}) = -9.03$
$Ca_f^{2+} + Sr^{2+} \Leftrightarrow Ca^{2+} + Sr_f^{2+}$	$\log(K_{Sr/Ca}) = 0.021$

2.2. Chemical model

Calcite dissolution, strontianite precipitation or dissolution and Ca^{2+}/Sr^{2+} cationic exchange on clays have been identified as the main reactions governing the strontium transport in the soil columns. In addition to these solid–solution interactions, the chemical model used in this work also includes both carbonic acid equilibria and water dissociation. Solutes of Ca and Sr are injected as chloride salts and Cl^- is considered to be a non-reactive species. Aqueous complexes of Ca^{++} or Sr^{++} with HCO_3^-, CO_3^{--} are not taken into account in this model and we verified that they were negligible as compared with free Ca^{++} and free HCO_3^-. Feeding solutions are in thermodynamic equilibrium with the atmospheric CO_2 before injection. However, there is no longer equilibration with the atmospheric CO_2 in the saturated porous medium. Phases are considered to be in a local thermodynamic equilibrium at a constant temperature (298 K). The speciation model is summarised in Table 3.

2.3. Transport model

The transport model is based on the assumptions that the fluid flow is steady and one-dimensional ($\vec{U}$ is the pore velocity of the fluid ($m\,s^{-1}$) corresponding to a fluid

Table 4
Hydrodynamic and physical characteristics of the column and fluid flow. V_p: porous volume; *CEC*: cation exchange capacity; *Pe*: Peclet number. The Peclet number can be interpreted as the ratio between advection and dispersion influences on solute transport. The high value observed here means that the transport of solutes in the column is dominated by advection

Diameter (mm)	Length L (mm)	Mass of sand (g)	V_p (ml)	*CEC* ($eq\,l^{-1}$)	Flow rate ($ml\,min^{-1}$)	$Pe = \dfrac{UL}{D}$
25.4	117	94	26	0.03	1	198

flow of $1\,ml\,min^{-1}$). The diffusion–dispersion factor, D ($m^2\,s^{-1}$), is constant. The Peclet number of the fluid flow,

$$Pe = \frac{UL}{D} \tag{1}$$

where L is the column length, is large (~ 200). This means that the transport of aqueous species is dominantly advective. The pore volume, V_p, and the Peclet number of the column, Pe, were determined experimentally by non-reactive tracer injections (Lefèvre et al., 1993). Table 4 summarises the main hydrodynamic parameters adopted for the computations.

3. The TRIO-EF and IMPACT migration codes

Both codes were run on an IBM RS6000 station with an AIX 3.2.5 operating system.

3.1. TRIO-EF

TRIO-EF is an object-oriented finite element code which is being developed at the CEA for the numerical modelling of thermohydraulic phenomena, atmospheric dispersion and hydrogeology. It is possible to simulate a stationary or transient fluid flow in one-, two- or three-dimensional space domains. Recent evolution of TRIO-EF in the field of earth sciences includes the development of an algorithm coupling solute transport by diffusion or advection with chemical transformations (Chupeau, 1991; Abdennour-Pfiffer, 1994). The user draws up his own instruction set and may include, if necessary, coupling with the evolution of temperature or permeability fields during the transport-chemistry calculations. The coefficient D is directly used as the dispersion operator in the transport equation. The chemical module used in TRIO-EF is derived from the geochemical code MINEQL (Westall et al., 1976; Schweingruber, 1984). At present, this equilibrium chemical model is able to take into account, in addition to the solution complexation and the dissolution–precipitation reactions, the sorption and ion exchange phenomena. The temperature dependence of equilibrium constants may be taken into account for space or time-dependent temperature fields. The ionic strength dependence of solute activity coefficients is described by the Davies approximation (Morel and Hering, 1993). The migration equations are solved by a two-step algorithm (Yeh and Tripathi, 1989; Abdennour-Pfiffer, 1994), in which the equations describing both transport and chemical speciation are solved iteratively between time step $p-1$ and time step p. At present, the reaction kinetics are not included in the model.

For the TRIO-EF calculations presented in this work, the maximal permitted values for dx ($dx = 0.6\,mm$) and dt ($dt = 8\,s$) imposed by U and D (Courant criterion: $U.dt/dx < 1$; Fourier criterion: $D.dt/(dx)^2 < 1$) were found to be inadequate to describe steep reaction fronts, such as those occurring at the head of the column. The predicted Sr distribution was found to be sensitive to the discretisation parameters

although dt and dx remained in the limits imposed by the Fourier and Courant criteria. Finite element discretisation, especially in the case of narrow concentration pulses which are in rapid advective motion, requires thus more restrictive limits on dt and dx. More satisfactory results were obtained by discretising the column in 234 elements of equal length ($dx = 0.5$ mm) with a lower and constant time step ($dt = 3$ s). An alternative but more complex discretisation scheme to this simple setting of dx and dt would have consisted in using a variable time and space discretisation. The boundary condition describing the input solution was applied to the first node of the column.

3.2. IMPACT

The IMPACT code is especially adapted for describing the transient transport of chemicals for various flow patterns with arbitrary chemical interactions. The description of chemical interactions is based on the concept of "phenomenological mechanisms" (Schweich et al., 1988). A phenomenological mechanism is composed of a set of stoichiometric relations, so-called elementary interactions, and the associated mass action laws assuming the phases are ideal. A simple activity correction is possible for ionic species in the aqueous phase only. The activity coefficient is calculated with the Güntelberg approximation (Cederberg et al., 1985). The basic assumptions include either an instantaneous local equilibrium, or mass transfer kinetic limitations, a steady flow, a constant temperature, a fixed pressure and a pore geometry.

IMPACT employs a model of mixing cells in series (MC model) to describe the flow in the column experiments. The dispersion process is represented by the model of mixing cells in series. The number of mixing cells, J, is directly linked to Pe by the relation (Villermaux, 1982):

$$Pe = 2(J - 1) \tag{2}$$

This model is an alternative to the standard continuous approach for modelling the one-dimensional advective–dispersive flow where the porous medium is represented by a continuous medium and dispersion is assumed to obey Fick's law with an appropriate dispersion coefficient. An adapted Newton–Raphson procedure is used to solve the algebraic equations obtained from the equilibrium calculation. The integration of differential mass balance equations is performed with the help of a predictor–corrector method with variable integration steps using the equilibrium constraints. In a new version of the code, it is possible to consider the chemical or physical kinetic limitations. The discrete MC model can be readily generalised to more complex stationary flow patterns, by using the ideal stirred reactor (mixing cell of uniform composition) as the basic element of a complex flow network (Jauzein et al., 1989).

As shown by Eq. (1) and Eq. (2), the number of mixing cells is directly linked to the dispersion coefficient and is determined to be $J = 100$ for the simulations presented in this work. Therefore, each cell represents a 1.17 mm column section. The time step is variable during computation, ranging from 0.1 s to about 30 s. In particular, time steps decrease strongly during the simulation stage where the dissolution of $SrCO_{3s}$ occurs (SOLEX experiment).

4. Comparison and discussion of the TRIO-EF and IMPACT predictions

4.1. SOLEX experiment (ion exchange and dissolution–precipitation)

Computation of this experiment shows that the initial injection of $SrCl_2$ leads to the formation of $SrCO_{3s}$ at the head of the column. The subsequent injection of $CaCl_2$ induces the dissolution of the $SrCO_{3s}$ precipitate and generates a strong Sr pulse which migrates through the column (Table 4 and Lefèvre et al., 1993). The evolution of the Sr concentration at the column outlet is represented as a function of the outflowing volume (equivalent to time) in Fig. 1(a). The TRIO-EF and IMPACT computations are in fair agreement with the experimental data. However, small differences between the TRIO-EF and IMPACT curves can be noted: (i) the maximum Sr concentration is observed slightly earlier with TRIO-EF, (ii) the maximum Sr concentration is 10% less in TRIO-EF's prediction than for IMPACT, and (iii) the Sr distribution is more spread out in time for TRIO-EF. In both cases, however, the ratio of the Sr breakthrough to the injected Sr, when the injected volume equals 8 times the porous volume V_p, is between 0.999 and 1. At the outlet of the column, the predicted evolutions of Cl^- concentration

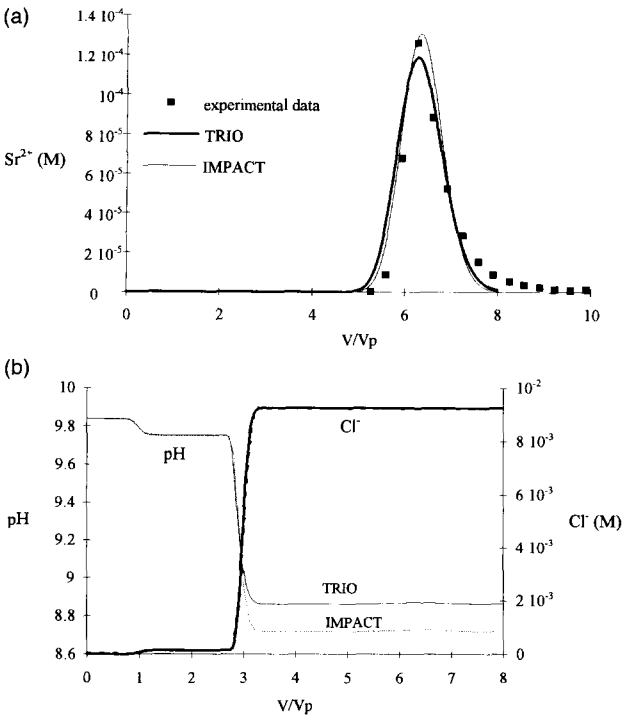

Fig. 1. SOLEX experiment: breakthrough curves. (a) Evolution of Sr^{2+} concentration at the column outlet as a function of injected volume—comparison between the experimental data, TRIO-EF and IMPACT simulations. (b) Comparison of TRIO-EF (solid line) and IMPACT (dotted line) predictions for Cl^- elution and pH at the column outlet. The pH discrepancy after $3V_p$ is about 0.15 pH units and originates from different treatments of activity coefficients for charged species by the two codes.

as a function of the injected volume are in very good agreement (Fig. 1(b)). The difference in pH curves after $3V_p$ (Fig. 1(b)) originates from the different treatment of activity coefficients of charged species in the IMPACT (no ionic strength correction) and TRIO-EF runs (Davies approximation for the activity coefficients). A rough correction made on the IMPACT simulation results accounted correctly for this pH gap. The simulations by the two codes for the distribution of the chemical species at the head of the column (first mixing cell for IMPACT, second node for TRIO-EF) as a function of delivered volume are also in good agreement (Fig. 2(a,b)): $SrCO_{3s}$ precipitates at the head of the column during the initial injection (see Table 1) and dissolves at the eluant change at $2V_p$. The differences in produced $SrCO_{3s}$ quantity and the time at which the precipitation starts are due to the difference in spatial discretisation in the two codes. According to the discretisation schemes adopted for the TRIO-EF and IMPACT simulations, the heads of the columns do not have equivalent "positions" and "volumes" in the two computations. Thus $SrCO_{3s}$ precipitates later in the IMPACT run and with a lower precipitation rate. This time difference is also observed on the sorbed Ca and Sr evolutions in Fig. 2(a). The distribution between sorbed and precipitated

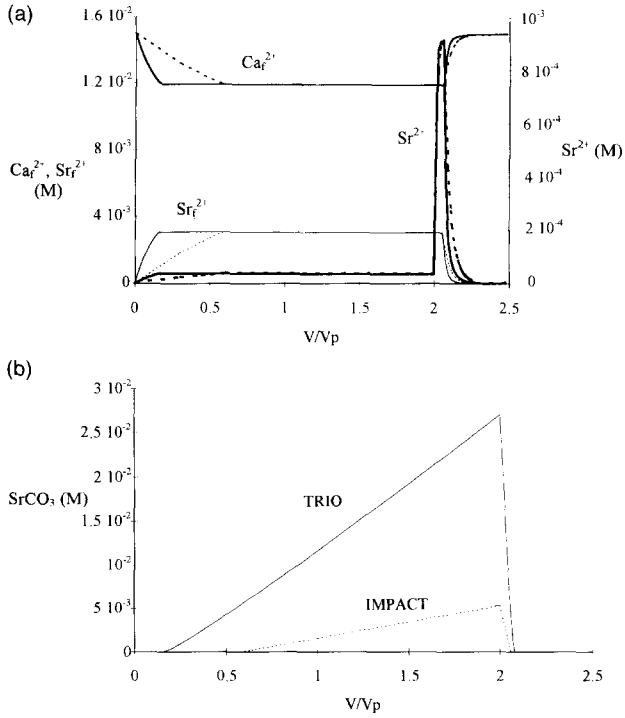

Fig. 2. SOLEX experiment, head of column: comparison between TRIO-EF (solid line) and IMPACT (dotted line). (a) Evolution of sorbed Ca and Sr (Ca_f^{2+}, Sr_f^{2+}) concentrations and aqueous Sr^{2+} concentrations at the head of the column as a function of the volume of injected solution (V_p = porous volume). (b) Evolution of the concentration of precipitated $SrCO_{3s}$ at the head of the column. Differences in the precipitation rates and the times at which precipitation starts in TRIO-EF and IMPACT are mainly due to the differences in spatial discretisation.

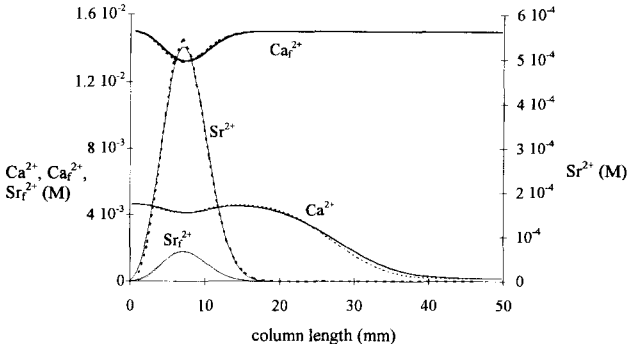

Fig. 3. SOLEX experiment: column profile at $2.23V_p$ after the beginning of the experiment (V_p = porous volume). Comparison between the predicted distributions of sorbed Sr and Ca (Ca_f^{2+}, Sr_f^{2+}) and aqueous Ca^{2+} and Sr^{2+} just after the $SrCO_{3s}$ precipitate has completely dissolved (TRIO-EF: solid line; IMPACT: dotted line).

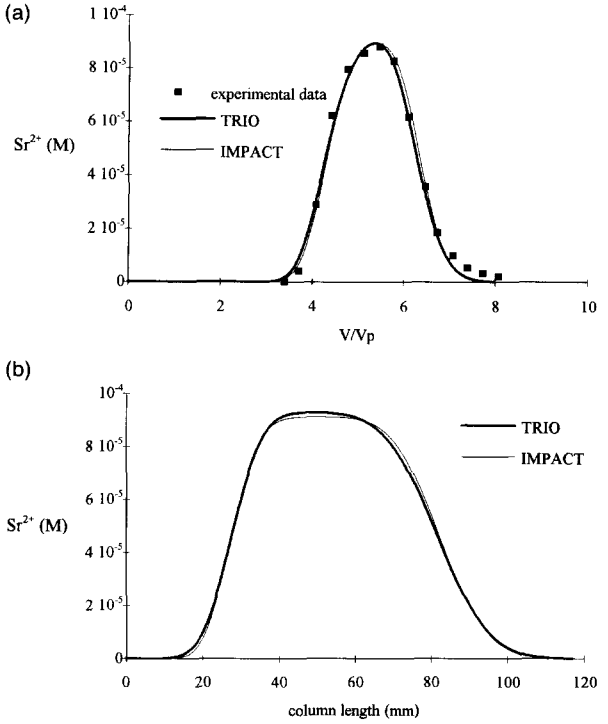

Fig. 4. IONEX experiment. (a) Evolution of Sr^{2+} concentration at the column outlet as a function of injected volume—comparison between the experimental data, TRIO-EF and IMPACT simulations. (b) Column profile after the injection of $3V_p$ of solution (V_p = porous volume). Comparison between the predicted distributions of Sr^{2+} for the TRIO-EF and IMPACT simulations.

strontium is therefore not exactly the same in the two simulations. Similarly, the redissolution of $SrCO_{3s}$ after $2V_p$ leads to the same time difference for the Sr desorption. Nevertheless, the predictions of final Sr breakthrough (Fig. 1) are close. Fig. 3 compares the spatial distribution of the chemical species in the column at a time corresponding to the injection of $2.23V_p$ of feeding solution, i.e. just after the dissolution of $SrCO_{3s}$. At this stage, the Sr^{++} pulses are in very good agreement. At the final breakthrough (Fig. 1(a)), larger differences between the two predictions for Sr^{++} are observed, probably originating from a slight numerical dispersion effect in TRIO-EF.

4.2. IONEX experiment (ion exchange—no precipitation)

In this experiment, there is no precipitation of $SrCO_{3s}$ and the retardation of Sr migration is only due to ion exchange phenomena (Table 1). The TRIO-EF and IMPACT predictions for the Sr elution are in very good agreement with the experimental data (Fig. 4(a)). Slight differences can however be noted: (i) the rise of the elution peak is about $0.05V_p$ earlier for TRIO-EF, and (ii) the maximum Sr^{++} eluted concentration is about 1% less in the TRIO-EF prediction. Fig. 4(b), which compares the TRIO-EF and IMPACT predictions for the spatial Sr^{++} distribution after the injection of $3V_p$ of solution, confirms the excellent agreement between both codes.

5. Conclusion

This migration code intercomparison exercise involved two codes which follow different approaches for modelling both solute transport and coupling of transport with chemical transformations. The agreement between these two codes, IMPACT and TRIO-EF, for the modelling of one-dimensional migration phenomena involving ion exchange, dissolution–precipitation and complexation reactions is nevertheless good. Both codes make predictions that are compatible with experimental data. Differences in the code predictions are often related to differences in the discretisation schemes. However, although the comparison of predictions for the migration of strongly reactive elements like Sr is fair (SOLEX experiment) or excellent (IONEX experiment), this exercise requires further numerical tests in order to clarify the origin of the slight discrepancies which are still unexplained. In particular, it would be interesting to evaluate the influence of the algorithm coupling transport and chemistry on the observed differences. Further intercomparison exercises are being prepared in relation to the experimental work on more complex chemical systems involving the migration of Cs and Np(V) typically.

References

Abdennour-Pfiffer, M., 1994. Etude hydrogéochimique et modélisation des phénomènes couplés transport-réactions liés au stockage de chaleur et/ou de déchets nucléaires dans les réservoirs géologiques. PhD thesis, Univ. Louis Pasteur, Strasbourg, France.

Cederberg, G.A., Street, R.L. and Leckie, J.O., 1985. A groundwater mass transport and equilibrium chemistry model for multicomponent systems. Water Resour. Res., 21: 1095–1104.

Chupeau, J., 1991. Contribution à l'étude théorique et expérimentale du transfert des solutés en aquifère: application au traçage chimique d'un réservoir géothermique, apports de la modélisation couplée transport-géochimie. PhD thesis, Univ. Pierre et Marie Curie, Paris, France.

Jauzein, M., Andre, C., Margrita, R., Sardin, M. and Schweich, D., 1989. A flexible computer code for modelling transport in porous media: IMPACT. Geoderma special issue, 44: 93–113.

Lefèvre, F., Sardin, M. and Schweich, D., 1993. Migration of strontium in clayey and calcareous sandy soil: Precipitation and ion-exchange. J. Contaminant Hydrol., 13: 215–229.

Morel, F.M.M. and Hering, J.G., 1993. Principles and applications of aquatic chemistry. Wiley, New York, 588 pp.

Schweich, D., Sardin M. and Jauzein, M., 1988. Consequence of physicochemistry on transient concentration wave propagation in steady flow. In: P.J. Wirenga and D. Bachelet (Editors), Proceedings of the International Conference and Workshop on the Validation of Flow and Transport Models for the Unsaturated zone, La Cruses, NM. State University Pub., pp. 370–380.

Schweingruber, M., 1984. User's guide for extended MINEQL (EIR Version). Technical Note EIR AN-45-84-39, Swiss Federal Institute for Reactor Research.

Villermaux, J., 1982. Génie de la réaction chimique: conception et fonctionnement des réacteurs. Lavoisier Tec. and Doc., Paris, 401 pp.

Westall, J.C., Zachary, J.L. and Morel, F.M.M., 1976. MINEQL, a computer program for the calculation of chemical equilibrium composition of aqueous systems. Technical Note No. 18, Dept. of Civil Engineering, MIT.

Yeh, G.T. and Tripathi, V.S., 1989. A critical evaluation of recent developments in hydrogeochemical transport models of reactive multichemical components. Water Resour. Res., 25: 93–108.